



Aalborg Universitet

AALBORG UNIVERSITY  
DENMARK

## Optimal Configuration and Sizing of Seaport Microgrids including Renewable Energy and Cold Ironing—The Port of Aalborg Case Study

Bakar, Nur Najihah Abu; Guerrero, Josep M.; Vasquez, Juan C.; Bazmohammadi, Najmeh; Othman, Muzaidi; Rasmussen, Brian Dalby; Al-Turki, Yusuf A.

*Published in:*  
Energies

*DOI (link to publication from Publisher):*  
[10.3390/en15020431](https://doi.org/10.3390/en15020431)

*Creative Commons License*  
CC BY 4.0

*Publication date:*  
2022

*Document Version*  
Publisher's PDF, also known as Version of record

[Link to publication from Aalborg University](#)

*Citation for published version (APA):*

Bakar, N. N. A., Guerrero, J. M., Vasquez, J. C., Bazmohammadi, N., Othman, M., Rasmussen, B. D., & Al-Turki, Y. A. (2022). Optimal Configuration and Sizing of Seaport Microgrids including Renewable Energy and Cold Ironing—The Port of Aalborg Case Study. *Energies*, 15(2), [431]. <https://doi.org/10.3390/en15020431>

### General rights

Copyright and moral rights for the publications made accessible in the public portal are retained by the authors and/or other copyright owners and it is a condition of accessing publications that users recognise and abide by the legal requirements associated with these rights.



- Users may download and print one copy of any publication from the public portal for the purpose of private study or research.
- You may not further distribute the material or use it for any profit-making activity or commercial gain
- You may freely distribute the URL identifying the publication in the public portal -

### Take down policy

If you believe that this document breaches copyright please contact us at [vbn@aub.aau.dk](mailto:vbn@aub.aau.dk) providing details, and we will remove access to the work immediately and investigate your claim.

## Article

# Optimal Configuration and Sizing of Seaport Microgrids including Renewable Energy and Cold Ironing—The Port of Aalborg Case Study

Nur Najihah Abu Bakar <sup>1,2,\*</sup> , Josep M. Guerrero <sup>1,\*</sup> , Juan C. Vasquez <sup>1</sup>, Najmeh Bazmohammadi <sup>1</sup> , Muzaidi Othman <sup>2</sup>, Brian Dalby Rasmussen <sup>3</sup> and Yusuf A. Al-Turki <sup>4</sup>

- <sup>1</sup> Center for Research on Microgrids (CROM), AAU Energy, Aalborg University, 9220 Aalborg, Denmark; juq@energy.aau.dk (J.C.V.); naj@energy.aau.dk (N.B.)
  - <sup>2</sup> Faculty of Electrical Engineering Technology, University Malaysia Perlis (UniMAP), Kampus Pauh Putra, Arau 02600, Perlis, Malaysia; muzaidi@unimap.edu.my
  - <sup>3</sup> Port Facility and Environment Management, Port of Aalborg, Langerak 19, 9220 Aalborg, Denmark; bdr@portofaalborg.com
  - <sup>4</sup> Center of Research Excellence in Renewable Energy and Power Systems, Department of Electrical and Computer Engineering, Faculty of Engineering, K. A. CARE Energy Research and Innovation Center, King Abdulaziz University, Jeddah 21589, Saudi Arabia; yaturki@kau.edu.sa
- \* Correspondence: numbab@energy.aau.dk or numajihah@unimap.edu.my (N.N.A.B.); joz@energy.aau.dk (J.M.G.)



**Citation:** Bakar, N.N.A.; Guerrero, J.M.; C. Vasquez, J.; Bazmohammadi, N.; Othman, M.; Rasmussen, B.D.; Al-Turki, Y.A. Optimal Configuration and Sizing of Seaport Microgrids including Renewable Energy and Cold Ironing—The Port of Aalborg Case Study. *Energies* **2022**, *15*, 431. <https://doi.org/10.3390/en15020431>

Academic Editor: Miguel Jiménez Carrizosa

Received: 19 October 2021

Accepted: 4 January 2022

Published: 7 January 2022

**Publisher's Note:** MDPI stays neutral with regard to jurisdictional claims in published maps and institutional affiliations.



**Copyright:** © 2022 by the authors. Licensee MDPI, Basel, Switzerland. This article is an open access article distributed under the terms and conditions of the Creative Commons Attribution (CC BY) license (<https://creativecommons.org/licenses/by/4.0/>).

**Abstract:** Microgrids are among the promising green transition technologies that will provide enormous benefits to the seaports to manage major concerns over energy crises, environmental challenges, and economic issues. However, creating a good design for the seaport microgrid is a challenging task, considering different objectives, constraints, and uncertainties involved. To ensure the optimal operation of the system, determining the right microgrid configuration and component size at minimum cost is a vital decision at the design stage. This paper aims to design a hybrid system for a seaport microgrid with optimally sized components. The selected case study is the Port of Aalborg, Denmark. The proposed grid-connected structure consists of renewable energy sources (photovoltaic system and wind turbines), an energy storage system, and cold ironing facilities. The seaport architecture is then optimized by utilizing HOMER to meet the maximum load demand by considering important parameters such as solar global horizontal irradiance, temperature, and wind resources. Finally, the best configuration is analyzed in terms of economic feasibility, energy reliability, and environmental impacts.

**Keywords:** cold ironing; energy management system; optimal sizing; renewable energy sources; seaport microgrids; maritime; HOMER

## 1. Introduction

Ports worldwide have different sizes, operations, geological, geographical features, and a variety of energy sources that will affect their power demand as well as energy production. The main sources of energy supply come from the utility grid and diesel generators, constantly emitting greenhouse gas emissions. Moreover, the energy sector is encountering primary energy depletion, considering that the growing load demand is exceeding power generation. With a rising awareness of the jeopardy from resource depletion issues and environmental pollution, many ports around the world are taking action toward the zero-carbon footprint goal. The urge to use alternative clean energy resources makes microgrids one of the best solutions for future green seaports. In 2019, Denmark showed a remarkable result by generating half of its electricity from wind and solar power [1]. The advantage of the climate's constant breezes and bluster in this country makes the wind turbine practical for use and well established. The Danish maritime

industry has set a target of 70% reduction in CO<sub>2</sub> emission by implementing wind energy and energy management systems in the ports [2].

Although microgrids are widely used in different land applications, there are limitations for their real implementation in the seaport sector. This situation is a good opportunity to introduce microgrids into the seaports, but at the same time it is challenging to access the references in terms of system requirements, optimal framework, stability, and maintenance needs. Especially during the initial planning phase, it is a vital task to find the optimal design of the seaport microgrid with a compatible configuration and the right sizing for each component.

In recent years, a lot of effort has been devoted to the optimal design of microgrids. Di Wu et al. [3] conduct a study on a two-stage stochastic mixed-integer programming technique for finding the optimal size of multiple distributed energy resources (DERs). The proposed model considers the optimal outcome in terms of economic benefits and system resilience. A comparative study in [4] evaluates the optimal framework for a standalone microgrid by using four different metaheuristic algorithms. The merit of the study is taking into account the uncertainty in RES power production and load consumption. Moreover, a sensitivity analysis for several battery prices and capacities is provided to find the best framework. The same technique is applied in [5] but with a three-level planning framework for the extreme event cases in a microgrid power system. The purpose of the study is to preserve system security for better power delivery. Furthermore, although numerous studies are available for the optimal sizing of batteries for microgrids, the battery sizing problem is still far from being mature. Different research strategies and schemes are applied in [6–10] to identify the optimal design for ESSs. Despite extensive research on design and optimal sizing of microgrid technologies in various applications, there is still a shortfall of this research in seaport microgrids. As the seaport itself is a very complex system consisting of various dynamic loads in different regions (shore and seaside), the maritime industry has traditionally been slow and reluctant in acknowledging this technology. However, seaport microgrids have been attracting a great deal of attention over recent years to improve maritime power systems' performance.

Therefore, this paper presents a simulation-based method using the HOMER optimizer to investigate the seaport microgrids configuration and sizing problem in terms of cost minimization, energy production, and environmental impact. Seaport microgrids in this paper refer to the integration of microgrid power systems into seaports with cold ironing facilities.

The evolvement of trading activities worldwide is increasing the reliance on maritime transportation. This situation resulted in the growing concern about the carbon footprint of ships when docked at ports [11]. When a ship is at berth, the auxiliary engine keeps on to supply onboard power demand [12]. It consumes a huge amount of heavy diesel oil depending on the berthing hours and ship's power requirement that emits hazardous gases and degrades air quality. Hence, ships' electrification alternative comes to the scene to reduce the air pollution during berthing by using cold ironing technology. Cold ironing is an emission-free technology that prevents vessels from continuously burning fossil fuels by supplying onboard electric power directly from the onshore grid [13]. The auxiliary engine is turned off (cold process), but the ship can continue to operate normally since the switchboard draws the power from the shore side (ironing). There are three types of cold ironing topologies: (1) centralized cold ironing, (2) distributed cold ironing, and (3) DC distribution cold ironing [14]. According to D. Colarossi and P. Principi [15], the size of the ship power plant varies with the type of the ship, with a typical distributed power system of 400 V. On the shore side, ships are generally connected with a medium voltage (MV) of 6.6 kV/11 kV. In order to step down or step up to the desired voltage level, transformers play a vital role in the system. Nevertheless, there are some obstacles in terms of frequency where most of the ports use 60 Hz, whereas Europe and Asia's ports use 50 Hz [13]. When the frequency on the shore side and the frequency on the ship do not match, a frequency

converter is required. Figure 1 illustrates a typical cold ironing connection from the shore side to the shipside.

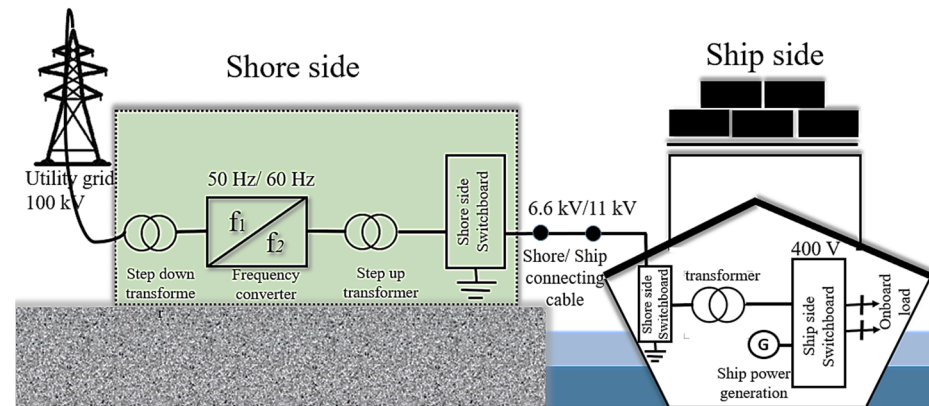


**Figure 1.** Typical cold ironing system from shore side to the seaside.

One of the challenges for port operation is the uncertainty in power demand, where the volume of traffic of berthing ships can suddenly change. Another scenario is the docking of large ships with heavy loads at the same time where the load demand might be larger than the available supply. Energy security to ensure the reliable port operation will be in low efficiency if cold ironing solely depends on the grid supply. These challenges are main motivations of this paper for investigating seaport microgrids with cold ironing facilities.

The emerging concept of the microgrid into the cold ironing is beneficial for the maritime industry. Collaboration between these two electrification technologies provides seaports with several advantages including resiliency, emission control, and economics. Cold ironing can cause power disturbances if the continuous high demand from the ships during berthing overtakes the supply capacity that cold ironing can provide. In the case of power breakdown, many of the port operations will be affected, leading to losses of billions of dollars. In this case, local distributed energy from the seaport microgrid is capable to offer the required energy in time of stress [16], thereby increasing energy security and resiliency. In addition, seaport microgrids can achieve high levels of port electrification by embracing cold ironing technology which the grid is unable to support. In terms of emission control, cold ironing itself eliminates a portion of emission by shutting down the conventional auxiliary engines while docking [17]. Seaport microgrids result in more pollution reduction by providing zero-carbon power from renewable energy sources. Moreover, seaport microgrids are economically efficient to reduce ports' operation costs, decrease peak-hour demand, and have the potential to sell back energy to the grid in case of having excess power. The contribution of this paper is three-fold:

- First, this paper attempts to integrate two of the most noteworthy maritime electrification technologies (cold ironing and microgrid) to enhance the sustainability of seaports energy systems. Although the microgrid concept is widely used in land-based applications, this technology remains scarce for the seaport sector.
- Second, this paper presents an optimal design for the seaport microgrid with the least cost providing a comparative study between three models.
- Third, in response to the three major concerns of the seaport sector, an optimal configuration for a seaport microgrid is provided with an analysis of economic feasibility, energy reliability, and environmental impacts. This analysis aims to investigate how integrating the microgrid concept into seaport applications may resolve the above-mentioned maritime issues.

The remainder of this paper is structured as follows. In Section 2, a review of the design optimization and sizing approaches for microgrids is provided. The methodology used for the design of the seaport microgrid, design parameters, and optimizer are introduced in

Section 3. Afterwards, the outcome from the proposed design is discussed and analyzed in Section 4. Finally, in Section 5, all significant findings of the paper are summarized.

## 2. Sizing

The optimal design and operation of microgrids have recently been the subject of extensive research. This is supported by an increasing trend of publications and research findings in this area. Ports are critical to the global economy, accounting for a big percentage of global trade and transportation. As a result, ports are preoccupied with providing labor for processing and handling goods, as well as other port-related services. Today's aggressive development in seaport trading necessitates an efficient power system capable of covering ports' electricity needs. Here, comes the concept of hybrid microgrid systems, in which the power generation is a mix of available clean energy sources with or without grid connection. The process to plan and develop this power system at seaports involves preliminary actions such as modeling, data collection, load and generation forecasting, initial simulation, evaluation, and performance assessment.

Sizing is a vital task to identify the optimal system configuration and the right capacity of the components to fulfill the load demand. Moreover, optimization is required to ensure that the system operates at high efficiency to maximize economic benefits while minimizing energy consumptions and environmental footprint. The study of microgrid systems in harbor areas by A. Roy et al. [18] emphasizes the importance of knowing the load demands and several evaluation criteria such as economic, pollution, and reliability, as well as geographical information to determine the sizing of the microgrid.

However, energy demands in seaports are highly dynamic and uncertain due to a variety of unpredictable factors such as the port's daily routine, activity handling, and environmental variables (weather conditions, temperature, and sea waves). Accordingly, there are sudden uncertain high loads that affect the stability of the system [19]. Considering this situation, ensuring the availability of power supply is significant to prevent disturbance in the maritime power system. P.Xie et al. [20] identify three common objectives and seven constraints of the seaport sector, which are summarized in Table 1. Based on the selected objectives and constraints, an optimization algorithm is developed and simulated to find the optimal design.

**Table 1.** Common objectives and constraints used in the port optimization problems.

Objectives	Constraints
<ul style="list-style-type: none"> <li>■ Fuel consumption minimization.</li> <li>■ Environmental footprint reduction.</li> <li>■ Economic investment minimization.</li> </ul>	<ul style="list-style-type: none"> <li>■ Power and energy balance.</li> <li>■ Restraints for power quality.</li> <li>■ Restraints of power plants.</li> <li>■ Restraints of ESSs.</li> <li>■ Environmental constraints.</li> <li>■ Ship voyage constraints.</li> <li>■ Constraints for the auxiliary system.</li> </ul>

For this purpose, both the computational resources and the required data related to the system are significant in the modeling phase. However, there are real-time data limitations, especially in the port sector. To overcome this challenge, computational simulation is a useful method to formulate and evaluate the microgrid performance before being implemented in real applications. The HOMER optimizer is one of the most widely used techniques in microgrid designs, which allows a flexible power system design with an integrated weather database for the RESs components. Table 2 presents an overview of the conducted studies on microgrid system designs using HOMER software in different sectors. Design objectives, system configuration, investigated sensitivity cases, site location, and the related sector are identified for each study.

**Table 2.** Summary of the Microgrid case study using HOMER optimizer. (Abbreviation: Photovoltaic (PV)).

References	Sector	Objectives	Configuration	Sensitivity Analysis	Case Study Location
[21] 2018	Residential Cottages	<ul style="list-style-type: none"> <li>- Cost and emission minimization</li> <li>- Nondervative optimization</li> </ul>	A standalone MG including PV, diesel generator, ac load, lead-acid battery, li-ion battery, and power converter	<ul style="list-style-type: none"> <li>- Fuel price</li> <li>- PV generation</li> </ul>	Kea, Greece
[22] 2020	General	<ul style="list-style-type: none"> <li>- Optimizing the size of the MG components</li> </ul>	A grid-connected MG including wind turbine, PV, battery, load, and power converter	N/A	Bahir Dar City, Ethiophia
[23] 2016	City, general	<ul style="list-style-type: none"> <li>- Optimal sizing</li> <li>- Optimal management of RESs and storage systems to fulfill the load demands and reduce the dependency on fossil fuels</li> </ul>	A standalone MG including wind turbine, PV, microturbine, battery, and fuel cell	N/A	Nain, Iran
[24] 2016	ATM machine	<ul style="list-style-type: none"> <li>- Feasibility analysis of solar- wind-diesel hybrid power system with maximum utilization of non-conventional generation systems while minimizing the total system cost</li> </ul>	A standalone MG including PV, wind turbine, diesel generator, power converter, battery, and ac load	N/A	Vatar, Kolhapur
[25] 2011	Forest	<ul style="list-style-type: none"> <li>- Analyzing real-time dynamic data</li> </ul>	A standalone MG including PV, wind turbine, hydro, diesel generator, power converter, battery, ac load, and fuel cell	<ul style="list-style-type: none"> <li>- Renewable resources</li> <li>- Hourly load data</li> <li>- PV array lifetime</li> </ul>	Kondapalli, India
[26] 2020	Rural area (residential)	<ul style="list-style-type: none"> <li>- Developing a microgrid, to explore the effect of certain problems such as power price, grid failure frequency, and grid mean repair time and studying its effects on cost (total operating cost, total capital cost, net present cost), electricity production, and unmet load</li> </ul>	A grid connected MG including PV and battery	<ul style="list-style-type: none"> <li>- Grid failure frequency</li> <li>- Grid mean repair time</li> </ul>	South Africa
[27] 2020	Agricultural Load (residential and water pumping)	<ul style="list-style-type: none"> <li>- Investigating the feasibility of the hybrid system</li> </ul>	A standalone MG including battery, PV, diesel generator, ac load, water pumping load, and power converter	<ul style="list-style-type: none"> <li>- Variations in PV cost</li> <li>- Diesel fuel price</li> <li>- Maximum annual capacity shortages (MACS)</li> </ul>	Ein Albaida, Palestine
[28] 2017	Remote area	<ul style="list-style-type: none"> <li>- To study two sizing methods for a standalone hybrid generation system using basic equations and Simulink Design Optimization (SDO) and HOMER optimizer</li> </ul>	A standalone MG including Hydrokinetic, PV, diesel generator, battery, and ac load	N/A	Isla Santay (Guayaquil)
[29] 2018	Seaport	<ul style="list-style-type: none"> <li>- Energy planning</li> </ul>	A grid-connected MG including PV, wind, battery, ac load, and power converter	N/A	Copenhagen, Denmark
[30] 2021	Domestic load	<ul style="list-style-type: none"> <li>- Minimizing the system cost</li> </ul>	A standalone MG Biomass, PV, wind, battery, dual power converter, electrical load, and dumb load	N/A	Yanbu, Saudi Arabia



This paper develops a simulation-based method to determine the best configuration and overall sizing for a hybrid generation system in a seaport microgrid by utilizing the HOMER optimizer. The flow of the proposed methodology from the MG structure design, parameter selection, simulation, and sensitivity analysis are given in the following sections.

### 3. Optimization Framework

#### 3.1. Structure of the Proposed Seaport Microgrid

In the proposed seaport microgrid design approach, RESs and ship demand during berthing are considered. The Port of Aalborg has been selected as a case study, which is located approximately at latitude  $57^{\circ}3.0'$  N and longitude  $10^{\circ}3.2'$  E, where energy sources mainly come from the utility grid, diesel generators, wind turbines (WTs), and PV systems. The Port of Aalborg handles a wide variety of goods and services such as container, cargo, railway, road, cruise, ships, and custom warehouse. However, in the modeling process, only the required power of ships during berthing is considered as it imposes a high energy demand on the port.

This paper aims to find the optimal seaport microgrid configuration and the optimal size of each component with the goal of cost minimization. Moreover, identifying the lowest net present cost (NPC) for the candidate architecture is a vital step in the seaport microgrid planning process. For instance, the payback period is very important for the investment by stakeholders as the energy consumption would be free during the rest of the project's lifetime. From the environmental perspective, RESs in microgrids provide the solution to the natural resources depletion issue and offer a green port landscape. Figure 2 illustrates the overview of the seaport microgrid configuration. The schematic design shows that the proposed system in this paper is connected with the main grid and consists of PV, WT, and a diesel generator, lithium-ion battery as a storage solution to complement RESs, a power converter between AC/DC busbars, and ships as electrical loads.

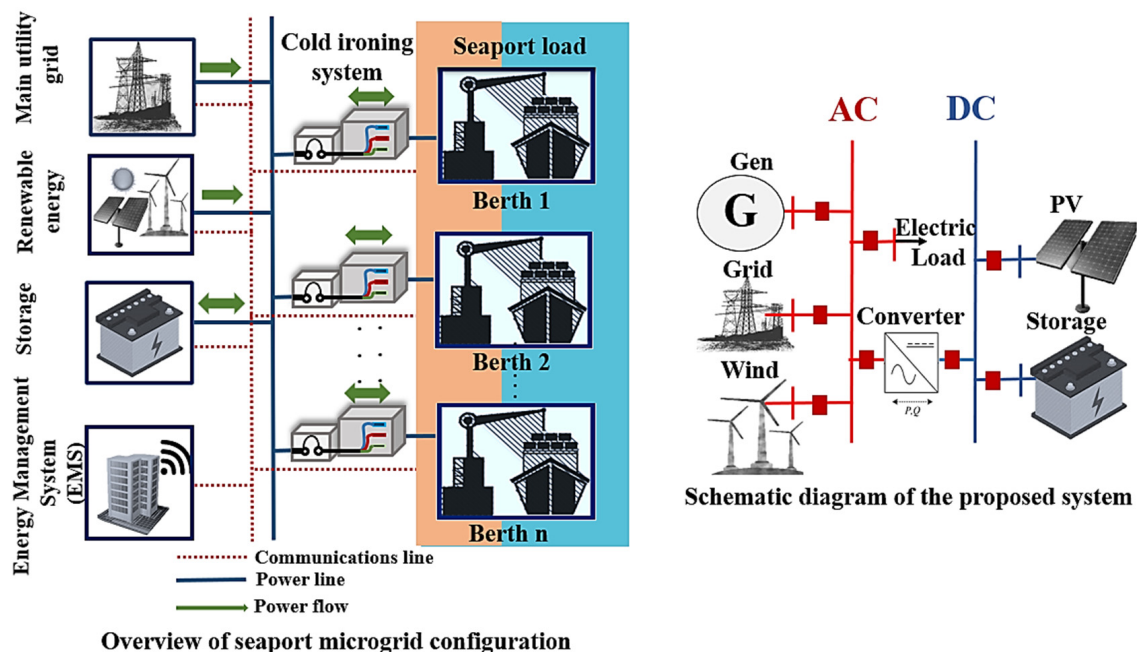


Figure 2. Overview and schematic diagram of the proposed system.

#### 3.2. Load Profile

In the Port of Aalborg, ships are among the big energy consumers. Conventionally, when a ship is at berth, the auxiliary engines are turned on to support some basic functions and auxiliary loads in the ship that need electrical power. However, burning fuel by diesel generators harms the environment. Nowadays, with the green maritime goals of the

shipping industry to reduce ship emission, cold ironing that also known as the onshore power supply (OPS) has come to the scene [31]. This technology allows ships to shut down their engines while berthed and plug into a power source at the shoreside [15]. In this way, ships have an adequate power supply to cover the onboard energy demand such as emergency equipment, cooling, heating, lighting, and refrigeration without the need to burn diesel fuels.

The load profile of ships during berthing varies according to three factors including time of berthing, the number of ships berthing per time, and the required power by a particular ship. There are different times of berthing for each ship and various numbers of ships berthing at the port from time to time. N. Ahamad et al. [32] summarize the average time of berthing and typical power requirement for different types of vessels, as listed in Table 3.

**Table 3.** Average berthing time and average power requirement for various types of vessels.

Type of Ships	Average Time Berthing (hrs)	Average Power
Chemical and other tankers	24–28	5 MW–6 MW
Bulk carrier	52	N/A
Container	21	1 MW–4 MW
General cargo	25	300 kW–6 MW
Ferries and RoRo	24	700 kW
Cruise	28	7 MW

The load profile used in the simulation in this study is shown in Figure 3. Peak hours are observed to be between 6 a.m. to 7 p.m. and the load slowly reduces afterward. According to this load profile, the average energy consumption is 23,977 kWh/day, which indicates that the average power per hour is 999.07 kW with a peak value of 2734.2 kW. Even though the power consumed by ships at the port depends on a few factors mentioned above during different periods and seasons of the year, it can be generally assumed that the peak load occurs during the afternoon as fewer ships are berthing between 8.00 p.m. and 5.00 a.m.

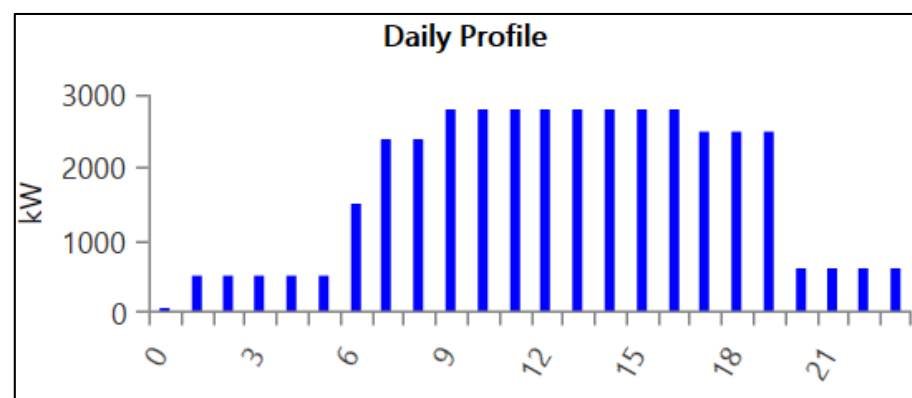


**Figure 3.** Hourly load profile in one day.

### 3.3. Meteorological Data

#### 3.3.1. Solar Radiation and Temperature

All the meteorological data used in this simulation such as solar global horizontal irradiance (GHI) data, wind resources, and temperature information are from the NASA Prediction of Worldwide Energy Resources (POWER) database. The extracted data are related to the site location specified by the port coordination so that the approximation of the WT and PV output power produced in the simulation will be more accurate. The bar chart in Figure 4 shows that the highest daily radiation readings occur in May, June, and August. It is because Denmark is in the midst of its summer season at the time. Most



of the days are sunny with a longer daylight period. Meanwhile, in other seasons, sun irradiation is low because it is cloudy and rainy most of the days. The irradiance ranges from 0.35 kWh/m<sup>2</sup>/day to 6.06 kWh/m<sup>2</sup>/day with an annual average of 3.02 kWh/m<sup>2</sup>/day. The orange line indicates that the maximum and the minimum clearness indexes are 0.55 and 0.338, respectively.

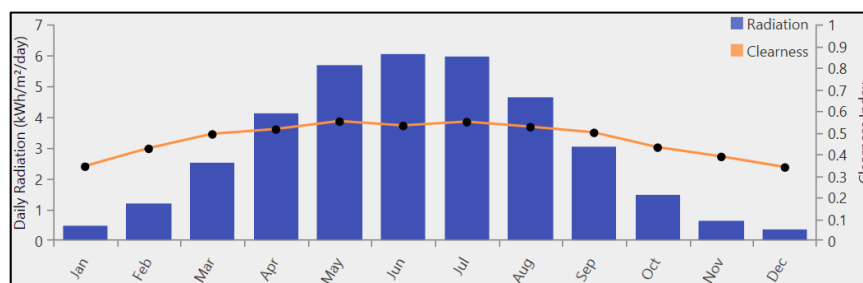


Figure 4. Solar GHI resources in one year.

The bar chart in Figure 5 displays the readings of the monthly average air temperature for this location. The range of temperature is between 0.94 °C and 16.66 °C with an annual average of 8.36 °C. The warmest months are June, July, August, and September, with an average temperature of 14.11 °C, 16.66 °C, 16.66 °C, and 13.44 °C, respectively. The temperature begins to fall sharply at the end of autumn and reaches its lowest point in February (0.94 °C).

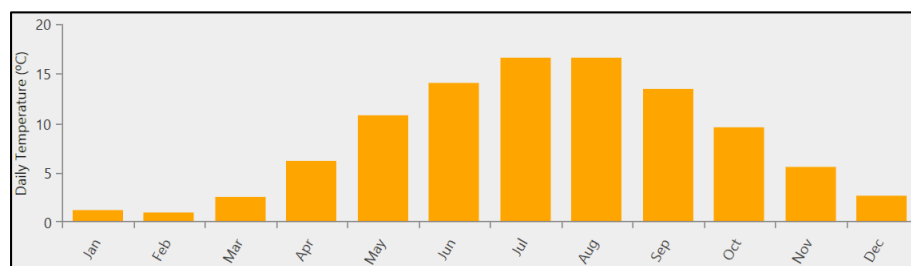


Figure 5. Average monthly temperature data of the target site in one year.

A. Haidar et al. [33] in their article highlighted that the generated power from PV modules is directly related to solar irradiance, temperature, the capacity of PV array, and its derating factor. This can be explained by Equation (1) that is used to determine the optimal capacity of the solar PV at time *t*.

$$P_{pv}(t) = P_{pv}^{ra}(t) \times f_{pv} \times \left( \frac{I}{I_e} \right) \times [1 + T_c (C_T - C_{Tc})] \tag{1}$$

where  $P_{pv}^{ra}(t)$  is the PV array rated capacity (kW),  $f_{pv}$  is derating factor,  $I$  is irradiance incident on PV plate (kW/m<sup>2</sup>),  $I_e$  is irradiance at the standard test condition (kW/m<sup>2</sup>),  $T_c$  is temperature coefficient,  $C_T$  is cell temperature, and  $C_{Tc}$  is cell temperature at the standard test condition.

### 3.3.2. Wind Resources

The power generation of WTs relies heavily on weather conditions such as wind speed and wind direction [34]. A common linear mathematical model for wind energy generation

estimation used to find the dynamical power curve of WTs output power is defined in Equation (2) [35]:

$$P_w(v) = \begin{cases} 0, & 0 \leq v \leq v_{in} \\ P_r \cdot \frac{v - v_{in}}{v_r - v_{in}}, & v_{in} \leq v \leq v_r \\ P_r, & v_r \leq v \leq v_{out} \\ 0, & v \geq v_{out} \end{cases} \quad (2)$$

where  $P_w(v)$  is the power output of the WT at wind speed  $v$ ,  $P_r$  is the WT rated power,  $v_r$  is the rated wind speed,  $v_{in}$  is cut-in wind speed, and  $v_{out}$  is cut-out wind speed.

Figure 6 illustrates the monthly average wind speed at the height of 50 m above the surface of the earth over one year period. The annual average wind speed is 8.17 (m/s), with the highest value of 9.62 (m/s) in January and the lowest value of 6.81 (m/s) in July. Due to the wind speed variation with height, it is plotted on a logarithmic scale. As can be seen in this figure, the wind speed increases with height because there are fewer obstacles and turbulence.

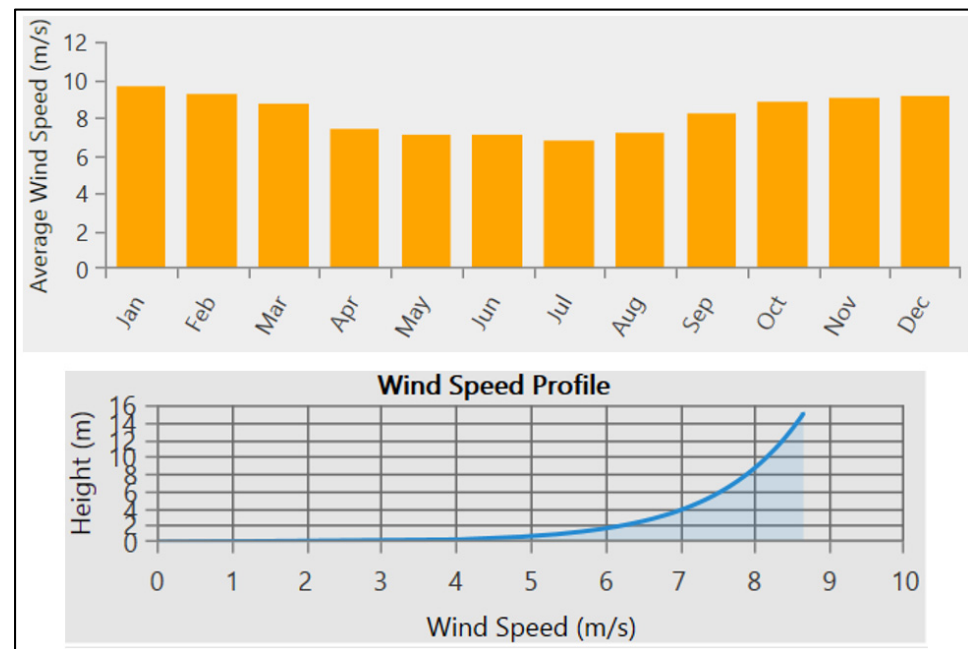


**Figure 6.** Wind speed profile of the target site in one year.

### 3.4. HOMER Optimizer

#### 3.4.1. Schematic and Design Parameters of the Proposed Seaport Microgrid

Hybrid Optimization of Multiple Energy Resources (HOMER) is a simulation-based software used to optimize any integrated system by finding the right size of the equipment and the best possible system configuration while minimizing the net present cost (NPC). It simulates the designed electric power system hour by hour for a year in the specific region considering the available energy resources present at the target location. For each time step, HOMER searches for many different configurations that satisfy the technical constraints at the lowest life cycle cost to meet the electrical load. Users can simulate their proposed power system and HOMER delivers the optimal candidate design.

Furthermore, it can perform sensitivity analysis to examine the impact of uncontrollable variables to see how they may affect the designed system costs. These variables include the price of fuel, which is always volatile, the price of components, lifetime data, efficiency, and other parameters that their change in the future is not known. Sensitivity analysis is critical for understanding the design's robustness. It enables users to be aware of how changing the input parameters affects the system architecture and cost.

Based on the proposed system in Section 3.1, the required components are added to the software. The schematic diagram of the system is shown in Figure 2. All the technical parameters and economic features are either from the software database or real data from commercial datasheets. Replacement cost is assumed to be 5–10% less than the capital cost.

### 3.4.2. Optimization Algorithm

HOMER has two optimization algorithms, which are: (1) the derivative-free algorithm and (2) the search algorithm. During the design process, the user may encounter a problem with determining the appropriate sizing or capacity for components that are compatible with the system. For the derivative-free algorithm, the software will automatically choose the appropriate sizing aiming for the least system cost. On the other hand, the search algorithm will simulate every possible system configuration by the quantity defined in the search space. The input value of the ‘search space’ varies depending on the peak load measurement. The selected size has a portion that is at the upper or lower end of the search space. It then specifies the best realizable system configuration capable of meeting the electric demand and finalizes it into a few categories. Table 4 shows the type of optimization option used for each of the components in this simulation.

**Table 4.** Optimization option used to determine the size for each component in the proposed design.

Component	HOMER Optimizer	Search Space
Diesel generator	✓	-
Wind turbine	-	5, 10, 15, 20, 25
PV	-	250, 500, 1000, 1500, 2000, 2500, 3000, 3500
Battery	✓	-
Converter	-	0~2880

The evaluation indices that are used in the software are net present cost (NPC), levelized cost of energy (COE), operating cost, and renewable fraction. The NPC or the life-cycle cost of a component is the present value of all the costs of establishing and operating every component in a system over the project lifetime, minus the present value of all the revenues that are earned over the project lifetime as shown in (3).

$$C_{NPC} = C_P - C_R \quad (3)$$

where  $C_P$  and  $C_R$  are the present values of all costs and revenues earned over the project lifetime, respectively.

Costs calculated in the algorithm include capital costs, replacement costs, O&M costs, fuel costs, emissions penalties, and the costs of buying power from the grid. Meanwhile, salvage value and grid sales income are included in the revenue. Overall, NPC is the HOMER’s main economic output which is used to rank all system configurations in the optimization results and is the basis from which the total annualized cost and the levelized cost of energy (COE) are calculated as follows:

$$COE = \frac{C_{ann,tot} - C_{boiler}H_{served}}{E_{served}} \quad (4)$$

where  $C_{ann,tot}$  is the total annualized cost of the system [USD/yr],  $C_{boiler}$  is the boiler marginal cost [USD/kWh],  $H_{served}$  and  $E_{served}$  are the total thermal and electrical loads served [kWh/yr], respectively. Meanwhile, to calculate the operating cost of the system, Equation (5) is utilized.

$$C_{operating} = C_{ann,tot} - C_{ann,capital} \quad (5)$$

where  $C_{ann,capital}$  is the total annualized capital cost [USD/yr]. To have an efficient system, it is highly recommended to include the RESs in the architecture. The renewable fraction used in the software refers to the percentage of the energy supplied to the loads that come from RESs. It can be calculated using the following equation:

$$f_{ren} = 1 - \frac{E_{nonren} - H_{nonren}}{E_{served} - H_{served}} \quad (6)$$

where  $E_{nonren}$  is nonrenewable electrical production [kWh/yr],  $H_{nonren}$  is nonrenewable thermal production [kWh/yr].

### 3.4.3. Mathematical Formulation of the Objective Function and Constraint

The objective of the optimization problem is to minimize the operation cost, as follows:  
Objective function:

$$\min(C_{total}) = \sum P_{grid}C_{grid} + P_{gen}C_{gen} + P_{WT}C_{WT} + P_{PV}C_{PV} + P_{bat}C_{bat} + P_{con}C_{con} \quad (7)$$

where the cost of each components includes capital cost, operation, maintenance, replacement, and fuel costs as given below:

$$C_{element} = \sum C_{capital} + C_{O\&M} + C_{replacement} + C_{fuel} \quad (8)$$

The objective function is subject to the power balance constraint between generation and demand and also the percentage of renewable energy.

Constraints:

$$P_{grid} + P_{gen} + P_{WT} + P_{PV} + P_{bat} + P_{con} \geq P_{load} \quad (9)$$

$$P_{WT} + P_{PV} \geq 60\% \quad (10)$$

### 3.5. Energy Management System (EMS) in the Design Phase

The complexity of multiple power resources coordination, varying electrical loads, fluctuation in economic variables, and assessing the environmental impact require the use of an EMS in both design and planning phases. EMS focuses on the use and coordination of energy sources over a specific time frame and is often combined with future forecasting and projection systems [20]. It is strongly related to both energy efficiency as well as cost savings. However, different functionalities and requirements can be defined for the EMS depending on the situation and the microgrid application.

In this design, three key concerns that are taken into account are the minimization of fuel consumption, environmental impact, and economic investment. The big question is what kind of system configuration and sizing specification should be considered. To satisfy this, RESs and storage elements are included in the design process. PVs and WTs in the schematic diagram represent the RESs; meanwhile, battery represents the storage component. The use of RESs will help to sustain the energy supply and its environmentally friendly characteristic will protect the environment from harmful emissions. Since the energy sources are from nature (sun and wind), RESs also provide the microgrids with a cost-effective power generation solution. Furthermore, any excess energy generated by RESs can be sold back to the grid bringing further economic benefits.

Utilization of the battery as an ESS is beneficial for both having an energy backup during critical periods (energy shortage and peak hours) and storing the excess energy when energy generation is abundant. RESs such as PV and WT have some limitations for power production. PVs are only able to generate power during the day, depending on solar radiation and temperature. PV power output is also reduced on cloudy and rainy days. The same situation exists for the WTs, where wind speed varies depending on the site location and seasonal wind patterns. ESS is a vital component to store excess energy from both solar and wind sources when they have high power generation and supply the

loads during periods of low energy availability, such as peak hours and power shortage intervals. Figure 7 illustrates how EMS plays part in the seaport microgrid system.

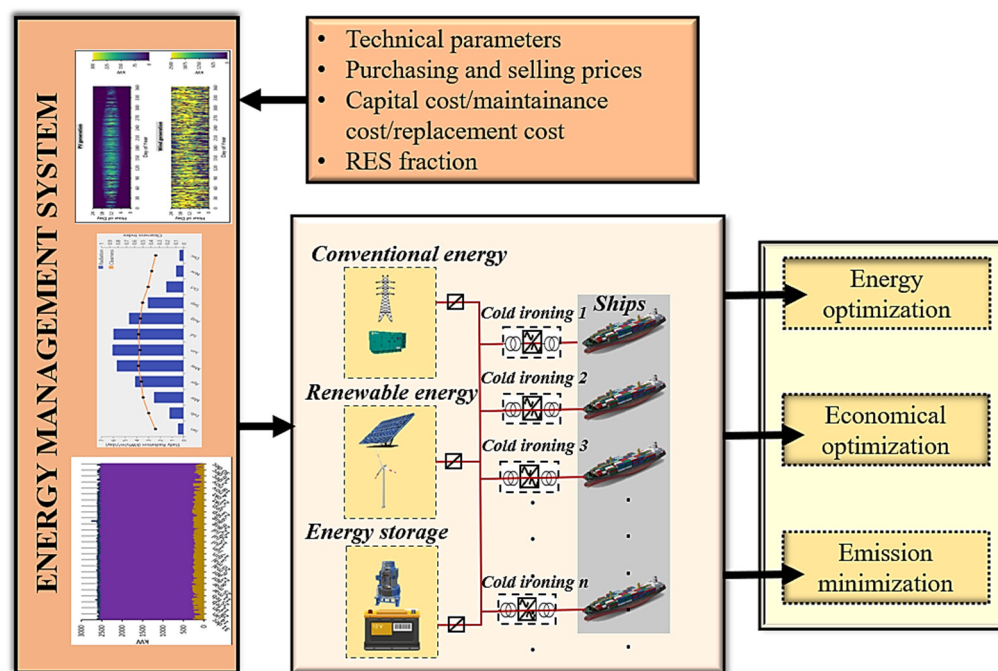


Figure 7. Energy Management System (EMS) in seaport microgrid.

#### 4. Optimal Sizing of Seaport Microgrid

In this section, three different models, namely, Model 1, Model 2, and Model 3, are investigated for the optimal hybrid seaport microgrid, where Model 1 is the proposed system, Model 2 is the best system recommended by HOMER, and Model 3 is a conventional system without a battery and RESs. Table 5 shows the detailed comparison between optimization results for Model 1, Model 2, and Model 3. All models are simulated during the 25-year lifetime of the project.

Table 5. Optimization results (All the data are retrieved from Homer Pro, accessed on 5 May 2021. Abbreviations: net present cost (NPC), levelized cost of energy (COE), renewable energy source (RES), Operation and Maintenance (O&M)).

Parameter	Proposed System (Model 1)	Optimal System (Model 2)	Conventional System (Model 3)
Configuration	Grid/Generator/PV/WT/Converter/Battery	Grid/PV/WT/Converter	Grid/Generator
Difference	-	-no battery -no diesel generator	-no RESs -no battery
PV (kW)	250	250	-
PV-MPPT (kW)	500	500	-
Wind turbine	25	25	-
Generator (kW)	3100	-	2800
Battery	1	-	-
Grid (kW)	999,999	999,999	999,999
Converter (kW)	90	90	-



Table 5. Cont.

Cost	NPC (USD)	5,920,870	4,718,247	26,981,960
	COE (USD)	0.0309	0.0246	0.2385
	Operating cost (USD/yr)	−42,392	−14,748	1,978,877
	Initial capital (USD)	6.47 M	4.91 M	1.4 M
System	RES frac (%)	85.2	85.2	-
	Total fuel (L/yr)	0	0	0
PV	Capital cost (USD)	300,000	300,000	-
	Production (kWh/yr)	315,315	315,315	-
Wind turbine	Capital cost (USD)	4,500,000	4,500,000	-
	Production (kWh/yr)	12,435,239	12,435,239	-
	O&M	125,000	125,000	-
Battery	Autonomy (h)	0.0801	-	-
	Annual throughput (kWh/yr)	320	-	-
	Nominal capacity (kWh)	100	-	-
	Usable Nominal Capacity (kWh)	80	-	-
Converter	Rectifier Mean Output (kW)	0.0385	0	-
	Inverter Mean Output (kW)	24.4	24.3	-
Grid	Energy purchased (kWh)	2,189,430	2,189,312	8,751,839
	Energy sold (kWh)	6,085,820	6,085,762	-
Emission	Carbon Dioxides (kg/yr)	1,383,720	1,383,645	5,531,162
	Sulfur Dioxide (kg/yr)	5999	5999	23,980
	Nitrogen Oxides (kg/yr)	2934	2934	11,727

Optimization results from the proposed design indicate that the best architecture for the target hybrid seaport microgrid is the grid/PV/WT/power converter configuration (Model 2) with the optimally sized components featuring the lowest NPC. The best system is selected based on the lowest value of NPC, which is USD 4,718,247 for Model 2, USD 5,920,870 for Model 1, and USD 26,981,960 for Model 3. The significant change that can be seen from Model 2 compared with the proposed system concerns its components where it has no diesel generator and battery.

Conventionally, without microgrid technology, the seaport sector relied only on the supply of electricity from the main grid and diesel generators to run their daily operation. According to Table 5, this architecture (Model 3) has the lowest initial capital cost, which is USD 1.4M, as the system does not need to invest in any other component such as RESs, ESSs, and power converters. Unfortunately, the system has the highest NPC value with USD 26M. The conventional system is highly dependent on the raw material of the power resources such as coal and diesel that produce very high greenhouse gas emissions. In terms of emission, this system produces 5,531,162 kg/yr of CO<sub>2</sub>, 23,980 kg/yr of SO<sub>2</sub>, and 11,727 kg/yr of NO<sub>x</sub>. Meanwhile, the hybrid microgrid system with optimal sizing in

Model 2 offers a big amount of emission reduction with a total reduction of 82.51% in CO<sub>2</sub>, 74.98% in SO<sub>2</sub>, and 74.98% in NO<sub>x</sub> compared with the conventional model. Significant emission reduction in Model 2 gives a positive impact to the environment toward achieving the green port goal. Besides producing hazardous pollutants, the conventional system also faces the problem of fossil resource depletion [36,37]. That explains, the reason why microgrid technology utilization is important for the seaport sector. The advantage of hybrid RESs and ESSs from microgrids will increase energy efficiency and provide sustainable energy while offering a long-term cost-effective solution for port electrification and decarbonization. This is supported by the significant amount of emission reduction in Model 1 and Model 2 that will certainly result in a better port environment.

According to the simulation results, the best architecture for the seaport microgrid in this project which is Model 2 consists of a 250 kW-PV, 25 100 kW-WTs, and a 90 kW-converter with a connection to the main grid. This microgrid requires 40,665 kWh/day and has a peak power demand of 2734 kW. The amount of excess electricity is 93,388 kWh/yr. Figure 8 shows the graph of energy production from both the utility grid and RESs that serve the electrical load. According to this figure, a big share of the produced power is related to RESs where 12,435,239 kWh/year is produced by the WTs, 315,315 kWh/year from PV, and only 2,189,312 kWh energy is purchased from the main grid. This indicates a RES fraction of 85.3%, whereas 14.7% of the power is from the main grid. The total energy production from PV, WT, and the main grid is equal to 14,939,866 kWh, from which 59% is used to supply the required power of the electrical loads (ships) and the remaining 41% of excess energy is sold back to the main grid. The amount of sold energy is 6,085,762 kWh, which is much higher than the energy purchased from the grid. In terms of emission, 1,383,645 kg/yr of CO<sub>2</sub>, 5999 kg/yr of SO<sub>2</sub>, and 2934 kg/yr of NO<sub>x</sub> are produced. The opportunity to gain extra money from selling back the energy to the main grid and reduce emissions compared with the conventional model is due to the deployment of RESs in the microgrid. Elimination of diesel generator and ESS in this model compared with the proposed system is due to the fact that power generation from RESs is more than enough to supply the current load. Thus, energy from the diesel generator and battery is not necessary in this case. Moreover, including a battery will increase the capital cost.

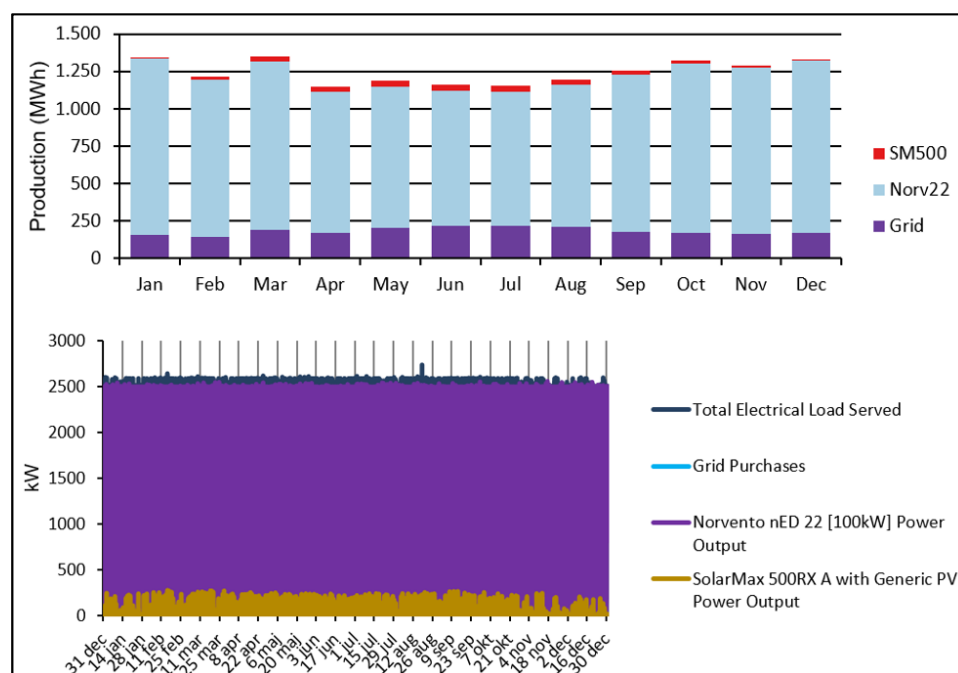


Figure 8. Energy generation and load consumption of Model 2.

Figure 9 shows both the PV and WTs power generation in Model 2 for a one-year duration. From the 85.3% of renewable energy fraction, 2.11% is from solar PV SM500 whereas the remaining 83.2% comes from Norv22 WT. The amount of energy produced by RESs and its reliability depend on the site location and the available natural resources. In this case study, Denmark as a seasonal country experiences high irradiation during the warm months (May, June, and July) due to the sunny climate and long hours of daylight. In those particular months, the output from the PV system is be higher compared with the power produced in other months with a high chance of having cloudy and rainy days. This limitation explains the reason for the small contribution of the PV system.

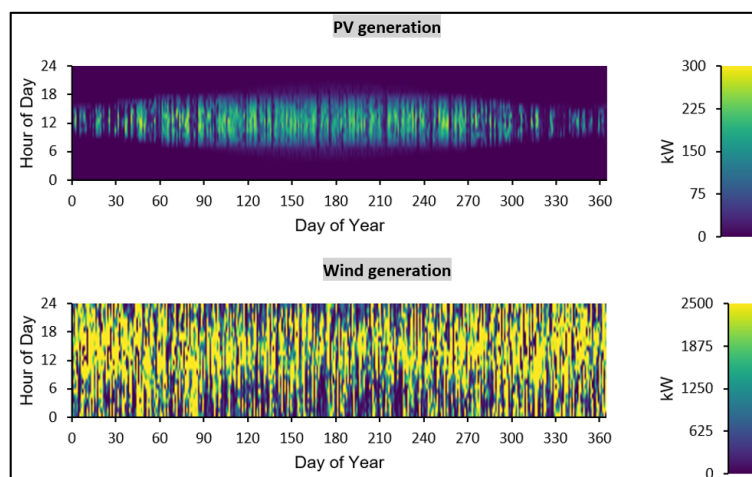


Figure 9. Solar and Wind generation of Model 2.

In the meantime, Denmark is a rich country in terms of wind resources as this country has relatively average wind speeds of 4.9–5.6 m/s measured at a height of 10 m. Denmark has vast offshore and onshore wind resources, as well as large swaths of sea territory with shallow water depths of 5–15 m, ideal for sitting WTs. Higher wind speeds, in the range of 7.08–9.62 m/s at 50 m height, are also available at these locations. There have been no big issues from wind variability.

A sensitivity analysis has been performed to evaluate the impact of the electricity price on the optimal system design. Four values of 0.20 USD/kWh, 0.4 USD/kWh, 0.6 USD/kWh, and 0.8 USD/kWh were evaluated. Table 6 summarizes the results obtained for various electricity rates loaded into the software. There is an increasing value of the NPC as the electricity rate increase. This is due to the growing share of the RES fraction and the requirement for more battery units to store the access energy from renewable sources. This makes sense considering that the optimizer is attempting to reduce the expenditure in electricity cost, hence increasing the utilization of power from RESs. In addition, as the RES fraction increases, a significant amount of emission is also reduced for CO<sub>2</sub>, SO<sub>2</sub>, and NO<sub>x</sub> gases.

Table 6. Sensitivity analysis of electricity price (all the data are retrieved from Homer Pro, accessed on 18 October 2021).

Electricity Price (USD/kWh)	Battery (Unit)	NPC USD	RES Fraction %	Emissions Production		
				CO <sub>2</sub> kg/yr	SO <sub>2</sub> kg/yr	NO <sub>x</sub> kg/yr
0.2	-	4.72 M	85.2	1,383,645	5999	2934
0.4	38	8.71 M	91.8	746,512	3236	1583
0.6	51	10.8 M	92.9	641,640	2782	1360
0.8	128	11.4 M	97.1	251,339	1090	533

## 5. Conclusions

This paper provided an optimal architecture for a seaport microgrid to support cold ironing services at ports. The design goal was to minimize the net present cost by optimizing the size of the components. A comparative discussion between a conventional seaport power system (grid/diesel generator) and two other hybrid designs of seaport microgrids was provided highlighting their difference in terms of cost, energy production, and emissions. The conclusion was that a grid/PV/wind/converter configuration with a 250 kW-PV, 25,100 kW-WTs, and a 90 kW converter with an NPC of USD 4,718,247 is the best seaport microgrid design to serve the given ship's load at the target port. More than 80% of electricity was generated from RESs, whereas only 14.7% of energy was purchased from the main grid. The proposed seaport microgrid was also able to sell a considerable amount of energy back to the main grid. In terms of emissions, the optimal design could offer a significant reduction in CO<sub>2</sub>, SO<sub>2</sub>, and NO<sub>x</sub> emissions, with a total reduction of 82.51%, 74.98%, and 74.98%, respectively. Emission reduction and cost-effectiveness of the optimal design of the seaport microgrid results in a promising solution for electrification of the future seaports following green maritime goals and the sustainable energy systems paradigm.

**Author Contributions:** Conceptualization, N.N.A.B.; software, N.N.A.B.; validation, N.B. and M.O.; formal analysis, N.N.A.B., visualization, N.N.A.B., writing—original draft preparation, N.N.A.B.; writing—review and editing, N.N.A.B. and N.B.; data provision, B.D.R.; supervision, J.M.G. and J.C.V.; project administration, J.M.G.; funding acquisition, Y.A.A.-T. All authors have read and agreed to the published version of the manuscript.

**Funding:** The Deanship of Scientific Research (DSR) at King Abdulaziz University, Jeddah, Saudi Arabia has funded this project, under grant no. (RG-49-135-40). The research work was also funded by a Villum Investigator grant (no. 25920) from The Villum Fonden.

**Institutional Review Board Statement:** Not applicable.

**Informed Consent Statement:** Not applicable.

**Data Availability Statement:** Not applicable.

**Acknowledgments:** This research work was supported by a Villum Investigator grant (no. 25920) from The Villum Fonden, University Malaysia Perlis, and Ministry of Education Malaysia. The Deanship of Scientific Research (DSR) at King Abdulaziz University, Jeddah, Saudi Arabia, has funded this project under grant no. (RG-49-135-40).

**Conflicts of Interest:** The authors declare no conflict of interest.

## References

1. Ministry of Foreign Affairs of Denmark. Pioneers in Clean Energy. Available online: <https://denmark.dk/innovation-and-design/clean-energy> (accessed on 13 May 2021).
2. Danish Port Targets 70 Percent Carbon Reduction Using Wind Energy. The Maritime Executive. 2021. Available online: <https://www.maritime-executive.com/article/danish-port-targets-70-percent-carbon-reduction-using-wind-energy> (accessed on 10 May 2021).
3. Wu, D.; Ma, X.; Huang, S.; Fu, T.; Balducci, P. Stochastic optimal sizing of distributed energy resources for a cost-effective and resilient Microgrid. *Energy* **2020**, *198*, 117284. [[CrossRef](#)]
4. Fathi, M.; Khezri, R.; Yazdani, A.; Mahmoudi, A. Comparative study of metaheuristic algorithms for optimal sizing of standalone microgrids in a remote area community. *Neural Comput. Appl.* **2021**, *6*, 1–19. [[CrossRef](#)]
5. Wang, Y.; Member, S.; Rousis, A.O.; Strbac, G. A Three-Level Planning Model for Optimal Sizing of Networked Microgrids Considering a Trade-Off Between Resilience and Cost. *IEEE Trans. Power Syst.* **2021**, *36*, 5657–5669. [[CrossRef](#)]
6. Gong, K.; Member, S.; Wang, X.; Jiang, C. Security-Constrained Optimal Sizing and Siting of BESS in Hybrid AC / DC Microgrid Considering Post-Contingency Corrective Rescheduling. *IEEE Trans. Sustain. Energy* **2021**, *12*, 2110–2122. [[CrossRef](#)]
7. Khezri, R.; Member, S.; Mahmoudi, A.; Member, S.; Haque, M.H.; Member, S. Sizing of Standalone Renewable-Battery Systems. *IEEE Trans. Sustain. Energy* **2021**, *12*, 2184–2194. [[CrossRef](#)]
8. Takano, H.; Hayashi, R.; Asano, H.; Goda, T. Optimal Sizing of Battery Energy Storage Systems Considering Cooperative Operation with Microgrid Components. *Energies* **2021**, *14*, 7442. [[CrossRef](#)]

9. Xie, C.; Wang, D.; Lai, C.S.; Wu, R.; Wu, X.; Lai, L.L. Optimal sizing of battery energy storage system in smart microgrid considering virtual energy storage system and high photovoltaic penetration. *J. Clean. Prod.* **2020**, *281*, 125308. [[CrossRef](#)]
10. Amini, M.; Khorsandi, A.; Vahidi, B.; Hosseinian, S.H.; Malakmahmoudi, A. Optimal sizing of battery energy storage in a microgrid considering capacity degradation and replacement year. *Electr. Power Syst. Res.* **2021**, *195*, 107170. [[CrossRef](#)]
11. Mueller, D.; Uibel, S.; Takemura, M.; Klingelhofer, D.; Groneberg, D.A. Ships, ports and particulate air pollution—An analysis of recent studies. *J. Occup. Med. Toxicol.* **2011**, *6*, 31. [[CrossRef](#)]
12. Abu Bakar, N.N.; Guerrero, J.M.; Vasquez, J.C.; Bazmohammadi, N.; Yu, Y.; Abusorrah, A.; Al-Turki, Y.A. A Review of the Conceptualization and Operational Management of Seaport Microgrids on the Shore and Seaside. *Energies* **2021**, *14*, 7941. [[CrossRef](#)]
13. Sciberras, E.A.; Zahawi, B.; Atkinson, D.J. Electrical characteristics of cold ironing energy supply for berthed ships. *Transp. Res. Part D Transp. Environ.* **2015**, *39*, 31–43. [[CrossRef](#)]
14. Sciberras, E.A. Shipboard Electrification—Emission Reduction and Energy Control. Ph.D. Thesis, Newcastle University, Newcastle, UK, 2016; p. 240.
15. Colarossi, D.; Principi, P. Technical analysis and economic evaluation of a complex shore-to-ship power supply system. *Appl. Therm. Eng.* **2020**, *181*, 115988. [[CrossRef](#)]
16. Abu Bakar, N.N.; Hassan, M.Y.; Sulaima, M.F.; Nasir, M.N.M.; Khamis, A. Microgrid and load shedding scheme during islanded mode: A review. *Renew. Sustain. Energy Rev.* **2017**, *71*, 161–169. [[CrossRef](#)]
17. Reusser, C.A.; Pérez, J.R. Evaluation of the Emission Impact of Cold-Ironing Power Systems, Using a Bi-Directional Power Flow Control Strategy. *Sustainability* **2020**, *13*, 334. [[CrossRef](#)]
18. Roy, A.; Auger, F.; Olivier, J.; Schae, E.; Auvity, B. Design, Sizing and Energy Management of Microgrids in Harbor Areas: A Review. *Energies* **2020**, *13*, 5314. [[CrossRef](#)]
19. Odun-ayo, T. Scholars' Mine Impact of Stochastic Loads and Generations on Power System Transient Stability. Ph.D. Thesis, Missouri University, Columbia, MO, USA, 2011; p. 58.
20. Xie, P.; Guerrero, J.M.; Tan, S.; Bazmohammadi, N.; Vasquez, J.C.; Mehrzadi, M.; Al-Turki, Y. Optimization-Based Power and Energy Management System in Shipboard Microgrid: A Review. *IEEE Syst. J.* **2021**, 1–13. [[CrossRef](#)]
21. Rousis, A.O.; Tzelepis, D.; Konstantelos, I.; Booth, C.; Strbac, G. Design of a Hybrid AC/DC Microgrid Using HOMER Pro: Case Study on an Islanded Residential Application. *Inventions* **2018**, *3*, 55. [[CrossRef](#)]
22. Yenalem, M.G.; Hinga, P. Modelling and Optimal Sizing of Grid-Connected Micro grid System using HOMER in Bahir Dar City, Ethiopia 2 Literature Review. *Int. J. Power Syst.* **2020**, *5*, 1–12.
23. Shahinzadeh, H.; Moazzami, M.; Fathi, S.H.; Gharehpetian, G.B. Optimal sizing and energy management of a grid-connected microgrid using HOMER software. In Proceedings of the 2016 Smart Grids Conference (SGC), Kerman, Iran, 20–21 December 2016; pp. 13–18. [[CrossRef](#)]
24. Kumar, P.; Pukale, R.; Kumabhar, N.; Patil, U. Optimal Design Configuration Using HOMER. *Procedia Technol.* **2016**, *24*, 499–504. [[CrossRef](#)]
25. Krishna, K.M. Optimization analysis of microgrid using HOMER—A case study. In Proceedings of the 2011 Annual IEEE India Conference, Hyderabad, India, 16–18 December 2011. [[CrossRef](#)]
26. Motjoadi, V.; Adetunji, K.E.; Joseph, P.K.M. Planning of a sustainable microgrid system using HOMER software. In Proceedings of the 2020 Conference on Information Communications Technology and Society (ICTAS), Durban, South Africa, 11–12 March 2020; pp. 1–5. [[CrossRef](#)]
27. Yasin, A.; Alsayed, M. Optimization with excess electricity management of a PV, energy storage and diesel generator hybrid system using HOMER Pro software. *Int. J. Appl. Power Eng. (IJAPE)* **2020**, *9*, 267–283. [[CrossRef](#)]
28. Lata-García, J.; Reyes-Lopez, C.; Jurado, F.; Fernández-Ramírez, L.M.; Sanchez, H. Sizing optimization of a small hydro/photovoltaic hybrid system for electricity generation in Santay Island, Ecuador by two methods. In Proceedings of the 2017 CHILEAN Conference on Electrical, Electronics Engineering, Information and Communication Technologies (CHILECON), Pucon, Chile, 18–20 October 2017; pp. 1–6. [[CrossRef](#)]
29. Ahamad, N.B.; Othman, M.; Vasquez, J.C.; Guerrero, J.M.; Su, C.-L. Optimal sizing and performance evaluation of a renewable energy based microgrid in future seaports. In Proceedings of the 2018 IEEE International Conference on Industrial Technology (ICIT), Lyon, France, 20–22 February 2018; pp. 1043–1048. [[CrossRef](#)]
30. Kharrich, M.; Kamel, S.; Alghamdi, A.; Eid, A.; Mosaad, M.; Akherraz, M.; Abdel-Akher, M. Optimal Design of an Isolated Hybrid Microgrid for Enhanced Deployment of Renewable Energy Sources in Saudi Arabia. *Sustainability* **2021**, *13*, 4708. [[CrossRef](#)]
31. Innes, A.; Monios, J. Identifying the unique challenges of installing cold ironing at small and medium ports—The case of aberdeen. *Transp. Res. Part D Transp. Environ.* **2018**, *62*, 298–313. [[CrossRef](#)]
32. Ahamad, N.B.B.; Guerrero, J.M.; Su, C.L.; Vasquez, J.C.; Zhaoxia, X. Microgrids Technologies in Future Seaports. In Proceedings of the 2018 IEEE International Conference on Environment and Electrical Engineering and 2018 IEEE Industrial and Commercial Power Systems Europe (EEEIC/I&CPS Europe), Palermo, Italy, 12–15 June 2018; pp. 1–6. [[CrossRef](#)]
33. Haidar, A.M.; Fakhar, A.; Helwig, A. Sustainable energy planning for cost minimization of autonomous hybrid microgrid using combined multi-objective optimization algorithm. *Sustain. Cities Soc.* **2020**, *62*, 102391. [[CrossRef](#)]
34. Ciulla, G.; D'Amico, A.; Di Dio, V.; Brano, V.L. Modelling and analysis of real-world wind turbine power curves: Assessing deviations from nominal curve by neural networks. *Renew. Energy* **2019**, *140*, 477–492. [[CrossRef](#)]



35. Wang, W.; Peng, Y.; Li, X.; Qi, Q.; Feng, P.; Zhang, Y. A two-stage framework for the optimal design of a hybrid renewable energy system for port application. *Ocean Eng.* **2019**, *191*, 106555. [[CrossRef](#)]
36. Zhou, Z.; Benbouzid, M.; Charpentier, J.F.; Scuiller, F.; Tang, T. A review of energy storage technologies for marine current energy systems. *Renew. Sustain. Energy Rev.* **2013**, *18*, 390–400. [[CrossRef](#)]
37. Brando, G.; Dannier, A.; Del Pizzo, A.; Di Noia, L.P.; Pisani, C. Grid connection of wave energy converter in heaving mode operation by supercapacitor storage technology. *IET Renew. Power Gener.* **2016**, *10*, 88–97. [[CrossRef](#)]